Cell Reports

Resource

Regional Cell-Specific Transcriptome Mapping Reveals Regulatory Complexity in the Adult *Drosophila* Midgut

Graphical Abstract

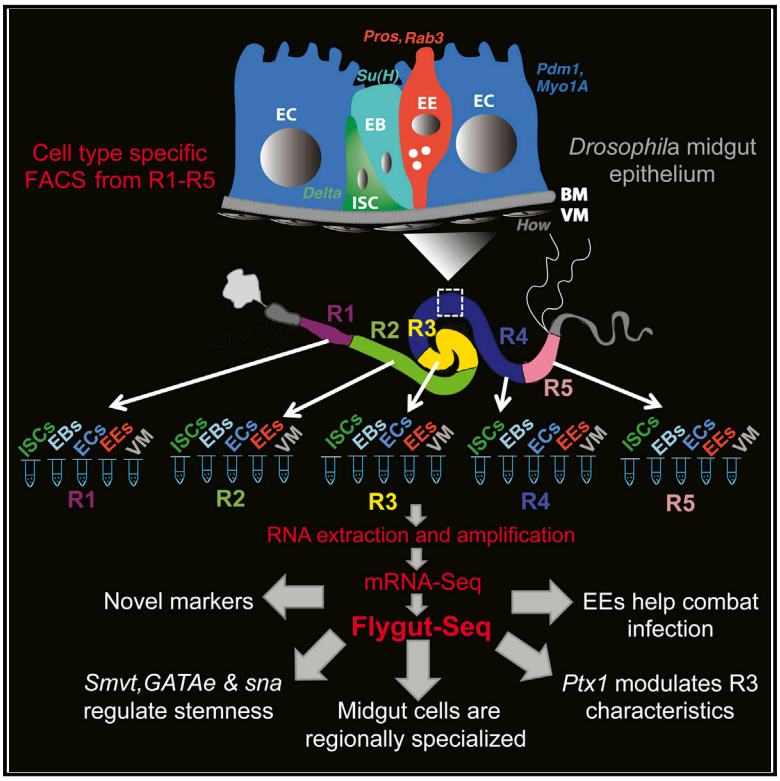

Highlights

- *Drosophila* intestinal cells are transcriptionally diverse across regions R1–R5
- *GATAe*, *sna*, and *Ptx1* are key players in global and regional ISC regulation
- Digestive enzymes are expressed cell type specifically in regions
- *P. entomophila* infection causes a massive transcriptional change in midgut cells

Authors

Devanjali Dutta, Adam J. Dobson, Philip L. Houtz, ..., Parthive H. Patel, Bruce A. Edgar, Nicolas Buchon

Correspondence

b.edgar@dkfz.de (B.A.E.), nicolas.buchon@cornell.edu (N.B.)

In Brief

In this study, Dutta et al. analyze the transcriptomes of *Drosophila* cells across five midgut regions (R1–R5) under physiological and infectious conditions. They identify markers and transcriptional factors regulating stem cells and regional specificities. This resource will be useful for studies on stem cells, regionalization, midgut homeostasis, and immunity.

Accession Numbers

GSE61361

Dutta et al., 2015, Cell Reports *12*, 346–358
July 14, 2015
http://dx.doi.org/10.1016/j.celrep.2015.06.009

CellPress

OPEN ACCESS
CellPress

Cell Reports
Resource

Regional Cell-Specific Transcriptome Mapping Reveals Regulatory Complexity in the Adult *Drosophila* Midgut

Devanjali Dutta,[1] Adam J. Dobson,[2,4] Philip L. Houtz,[2] Christine Gläßer,[1] Jonathan Revah,[2] Jerome Korzelius,[1] Parthive H. Patel,[1] Bruce A. Edgar,[1,3,*] and Nicolas Buchon[2,3,*]
[1]German Cancer Research Center (DKFZ), Center for Molecular Biology Heidelberg University (ZMBH) Alliance, Im Neuenheimer Feld 282, 69120 Heidelberg, Germany
[2]Department of Entomology, Cornell University, Ithaca, NY 14853, USA
[3]Co-senior author
[4]Present address: Institute of Healthy Ageing, University College London, London WC1E 6BT, UK
*Correspondence: b.edgar@dkfz.de (B.A.E.), nicolas.buchon@cornell.edu (N.B.)
http://dx.doi.org/10.1016/j.celrep.2015.06.009

SUMMARY

Deciphering contributions of specific cell types to organ function is experimentally challenging. The *Drosophila* midgut is a dynamic organ with five morphologically and functionally distinct regions (R1–R5), each composed of multipotent intestinal stem cells (ISCs), progenitor enteroblasts (EBs), enteroendocrine cells (EEs), enterocytes (ECs), and visceral muscle (VM). To characterize cellular specialization and regional function in this organ, we generated RNA-sequencing transcriptomes of all five cell types isolated by FACS from each of the five regions, R1–R5. In doing so, we identify transcriptional diversities among cell types and document regional differences within each cell type that define further specialization. We validate cell-specific and regional Gal4 drivers; demonstrate roles for transporter *Smvt* and transcription factors *GATAe*, *Sna*, and *Ptx1* in global and regional ISC regulation, and study the transcriptional response of midgut cells upon infection. The resulting transcriptome database (http://flygutseq.buchonlab.com) will foster studies of regionalization, homeostasis, immunity, and cell-cell interactions.

INTRODUCTION

The intestine is a dynamic organ composed of specialized cells that primarily perform the functions of digestion, absorption of nutrients and water, and expulsion of waste. It also serves as a major site of interaction with the external environment, which includes numerous microbes and chemicals. Fulfilling these multiple roles requires the gut to be a highly homeostatic organ that adapts in response to both extrinsic environmental cues and intrinsic organismal signals.

The adult *Drosophila* midgut undergoes constant development and renewal (Ohlstein and Spradling, 2006, 2007; Micchelli and Perrimon, 2006; Jiang et al., 2009, 2011; Buchon et al., 2009; Amcheslavsky et al., 2009). Intestinal stem cells (ISCs) express the Notch ligand *Delta* (*Dl*) and proliferate throughout adult life, renewing and generating transient bi-potent progenitors called enteroblasts (EBs). ISCs and EBs are characterized by expression of the transcription factor (TF) *escargot* (*esg*). Upon activation of the Notch receptor by Delta, EBs express the TF *Suppressor-of-hairless* (*Su(H)*) and differentiate predominantly into absorptive enterocytes (ECs) that express *Myosin1A* (*Myo1A*) and the POU domain TF *Pdm1* (or *nubbin*). However, some *Su(H)*$^{+}$ EBs also differentiate into class II enteroendocrine cells (EEs) that express the neuro-endocrine marker *Prospero* (*pros*) and a specific combination of neuropeptides such as *Tk* and *DH31* (Beehler-Evans and Micchelli, 2015). Distinct pros^{+} EEs, denoted as class I, express neuropeptides *Ast A*, *B* and arise from *Su(H)*$^{-}$ EBs, which have not registered Notch activation. Alternatively, it has recently been proposed that commitment to EE lineage is established in a subpopulation of ISCs that express *pros* (Biteau and Jasper, 2014; Zeng and Hou, 2015). The midgut is also surrounded by circular and longitudinal visceral muscles (VMs), which facilitate peristalsis and serve as a dynamic niche, secreting niche signals including Wg, the epidermal growth factor receptor (EGFR) ligand Vn, and the JAK-STAT ligand Upd1, together with adhesion molecules (e.g., integrins) (Lin et al., 2008; Jiang et al., 2011; Biteau and Jasper, 2011). In addition to these signaling pathways, JNK, Dpp, and Hippo signaling are all involved in regulating cell growth and ISC proliferation in the midgut (Shaw et al., 2010; Tian and Jiang, 2014; Guo et al., 2013). ISCs are also vital for sustaining tissue regeneration following injury, apoptosis, and pathogenic assaults (Buchon et al., 2010; Cordero et al., 2012). The digestive tract is thus a complex mix of cells of distinct identity, developmental origin, and differentiation states.

The adult *Drosophila* midgut has been described as being divided into three distinct compartments, namely the anterior, middle, and posterior regions, based largely on morphological differences (Dimitriadis, 1991). Recent studies have revealed

finer compartmentalization, dividing the midgut into five major regions (R1–R5, from anterior to posterior) that are transcriptionally, functionally, and morphologically distinct. These can be further sub-divided into 14 sub-regions (Buchon et al., 2013a; Marianes and Spradling, 2013). The latter two studies characterized gene expression differences among the five major midgut regions and noted compartmentalization of digestive, metabolic, and immune functions. However, cell-type-specific gene expression was not assayed in these studies. Nevertheless, regional variation within cell types is quite obvious in the fly's midgut. For instance, ISCs show clear regional differences in basal division rates and generate distinct regional subtypes of epithelial cells along the gut (Marianes and Spradling, 2013; Martorell et al., 2014). In the anterior-most region of the midgut (R1), type I gastric stem cells (GaSCs) have been shown to renew cells of the proventriculus, which is itself devoid of ISCs (Singh et al., 2011). The middle midgut (R3) is basally renewed at very low levels and is inhabited by a population of generally quiescent stem cells called type II GaSCs (Strand and Micchelli, 2011). Understanding region-dependent and cell-specific properties is key to understanding how the gut fulfills its physiological roles and maintains coordination and harmonious function in the face of environmental variation (e.g., pathogenic attacks or ingestion of food). Therefore, it is important to profile the various intestinal cell types at the transcriptome level so that they can be analyzed and manipulated more extensively.

Here, we present a comprehensive transcriptome resource of region-specific, cell-type-specific RNA-sequencing (RNA-seq) profiles of *Drosophila* midgut cell populations, including progenitors (ISCs and *Su(H)*$^+$ EBs), differentiated epithelial cells (ECs and EEs), and VMs, isolated using fluorescence-activated cell sorting (FACS) (Dutta et al., 2013). Using cell-type-specific genetic manipulations, we validate numerous predictions derived from our RNA-seq data. This transcriptome dataset and its associated online database at Flygut-seq (http://flygutseq.buchonlab.com) will be valuable resources that should help define the specialized functions of the different gut regions and facilitate future studies using the *Drosophila* midgut.

RESULTS

Drosophila Midgut Cells Are Transcriptionally Diverse

To investigate variation in gene expression between midgut cell populations across the five regions (R1–R5, Figure 1A), we marked each respective cell type with GFP using cell-type-specific Gal4-based transcriptional "drivers" to activate a Gal4-responsive transgene encoding GFP (*UAS-GFP*) as described in Experimental Procedures. Pure populations of all five midgut cell types from each of the five regions (R1–R5) were isolated using FACS, based on GFP intensity and cell size as determined by forward light scatter (FSC). RNA was extracted from each cell type of each region in biological duplicates, amplified, and subjected to mRNA sequencing. Raw fastq reads were mapped to the *Drosophila* genome using Tophat and reads were normalized per kilobase per million mapped reads (RPKM). For differential expression analysis, the DESeq package was used (see Experimental Procedures and Supplemental Experimental Procedures). Marker genotypes and the protocol used for profiling midgut cell types can be found in the Experimental Procedures. For simplicity, we refer to the *Su(H)*$^+$ cells as EBs throughout the text. Su(H)-EBs committed to enteroendocrine cell differentiation were not specifically profiled due to the lack of a suitable marker.

We first determined overall transcriptome differences between cell types by hierarchical clustering (Figure S1A). This indicated that the mesodermally derived VM had a dramatically different transcriptome compared to the endodermal cell types, suggesting that the embryonic origin of tissues can still be detected in the transcriptome of adult cells. Principal component analysis (PCA) explained ~35% of the total transcriptional variance in the first two principal components (PCs), distinguishing EEs as the most divergent endodermal cell population, potentially due to their neuronal properties (Figure 1B). EBs were more similar to ECs than some ISC populations, indicating as expected that *Su(H)*$^+$ EBs may be in the process of adopting the EC fate. *esg* marks both EBs and ISCs, and accordingly, the transcriptome of cells marked with *esg* overlapped with both profiles. As analyses encompassing partial overlapping cell populations would skew the results, we excluded the *esg*$^+$ cell profiles from subsequent statistical analyses. Because of its great divergence, we also analyzed VMs separately from other cell types. Data from *esg*$^+$ cells and VMs can be found in Flygut-seq.

We found more than 50% of protein-coding genes in the genome to be expressed in the adult midgut. Of these genes, ~40% (2,456) were differentially expressed (DE) among all four cell types (ISCs, EBs, ECs, and EEs) using a criterion of at least log2 fold change and a 5% false discovery rate (FDR) in a DE analysis (Table S1) (Anders and Huber, 2010). Unbiased hierarchical clustering ordered the samples according to their developmental progression from progenitors (ISCs and EBs) to differentiated cells (EEs and ECs). This was due to mostly non-overlapping expression between these two classes of cells, along with some cell-type-specific expression (Figure 1C). Gene Ontology (GO) enrichment analysis of the genes enriched in EEs revealed the high expression of G-protein-coupled signaling pathway components and neuropeptides, while ECs highly expressed serine endopeptidases and proteolytic genes (Figures S1B and S1C; Table S2).

Applying a metric of $\geq$2-fold difference in mean expression among the four cell types, we identified 159 genes that were enriched at least 2-fold in ISCs (ISC-high) and 509 genes that showed extremely low expression in ISCs (by $-$1- to $-$10-fold) compared to other epithelial cell types (Table S1). Stem cell-high genes included the known ISC markers *Delta*, *arm*, *mira*, and *Robo2/lea* (Bardin et al., 2010; Biteau and Jasper, 2014) and sequence-specific DNA binding TFs such as *sc*, *dys*, *snail* (*sna*), and *ap* (Table S1). GO analysis (Figure 1D; Table S2) revealed that the ISC-high genes were enriched for functions in cell-cycle regulation and stem cell proliferation. This trend was driven by high expression of genes including *polo, cdc2*, *mad2*, *tum*, and *Cks30A*, consistent with the fact that ISCs are the only multipotent actively mitotic cell population in the *Drosophila* midgut. Interestingly, genes involved in fate decisions and asymmetric stem cell division in neuronal progenitors, such as *pon*, *mira*, *bora*, and *jumu*, were also highly expressed in ISCs.

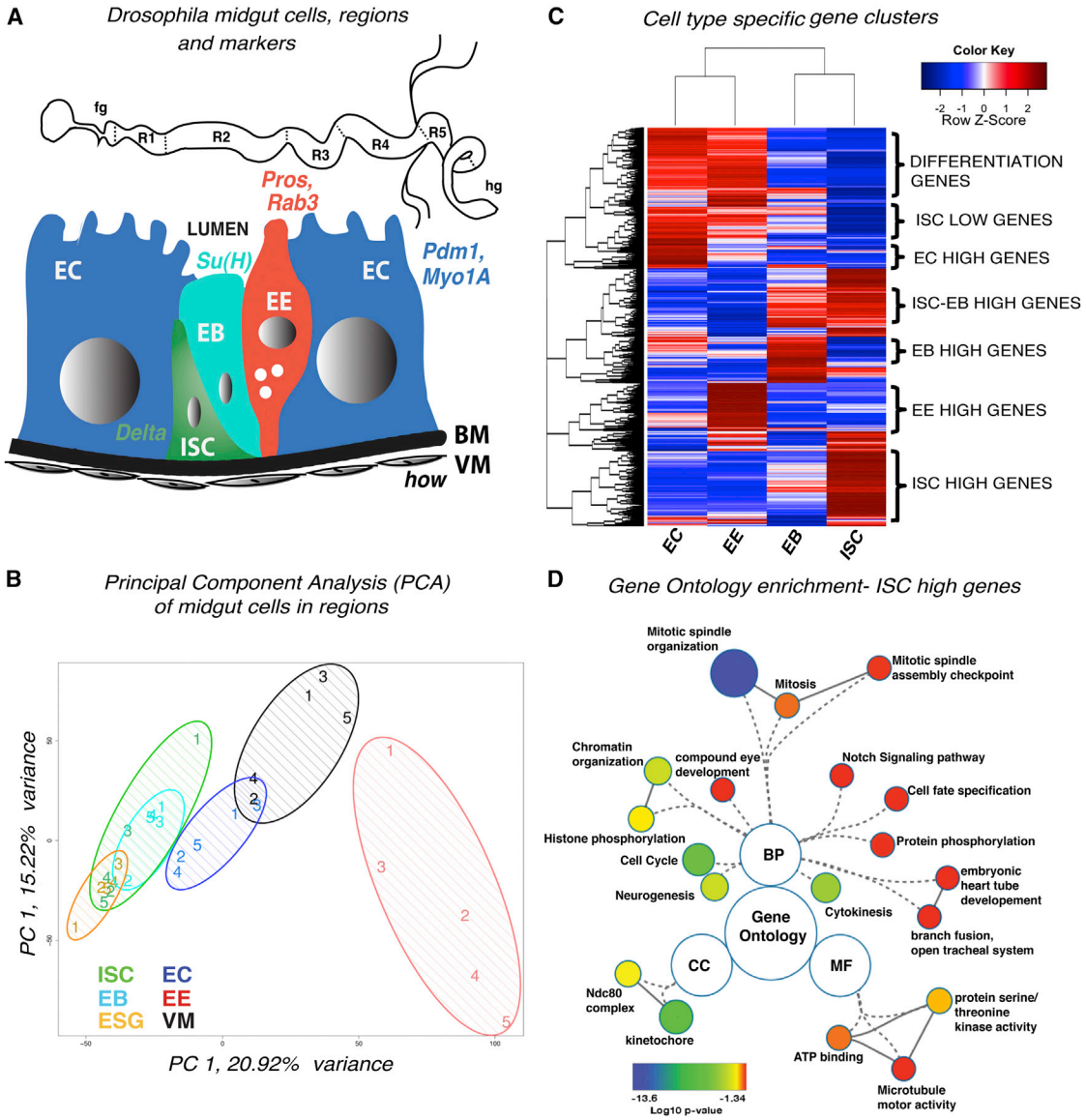

Figure 1. *Drosophila* Midgut Cells Are Transcriptionally Dynamic

(A) Diagrammatic representation of the adult *Drosophila* midgut cells, cell-type marker genes, and regions. R1–R5: regions of the midgut, fg: foregut, hg: hindgut, BM: basement membrane.

(B) PCA (mean of all replicates) showing EEs are distant from other endodermal cell types. Numbers depict regions R1–R5.

(C) Normalized RPKM heatmap of differentially expressed genes (Table S1) (physiological and regions) shows cell type specific gene clusters. (Scale: Normalized expression values increasing from blue to red. Scaling of matrices by row to a mean of 0 and SD of 2 (Z score normalization) shows relative expression patterns.)

(D) GO enrichment plot of ISC-high genes. Scale and size of balls represents p value. BP, biological processes; MF, molecular functions; CC, cellular components.

Accordingly, ISCs have been reported to divide asymmetrically in 79% of divisions (Goulas et al., 2012). Genes involved in chromatin organization and histone modification, such as *ball*, *aurB*, and *Df31*, were also highly upregulated in ISCs. Using gene and protein traps, we validated the expression patterns of a number of ISC-high genes, verifying them to be highly expressed in ISCs (Figure S1D).

To understand the progressive changes in gene expression that occur as differentiation proceeds, we followed the expression patterns of the 2,456 differentially expressed genes and found that the expression of 181 genes progressively increased as differentiation proceeded from ISCs to EBs to ECs, including genes involved in proteolysis, *Ser6* and *ζTrypsin*, mucins such as *Mucin-68E*, and the oxidative stress response gene *GstE9* (Table S3). Only 41 genes decreased in expression from ISCs to EBs to ECs, including the TF *sna* and epigenetic factors *piwi* and *zuc* (Table S3), suggesting that these genes could be required for stem cell maintenance and/or that their repression in EBs might

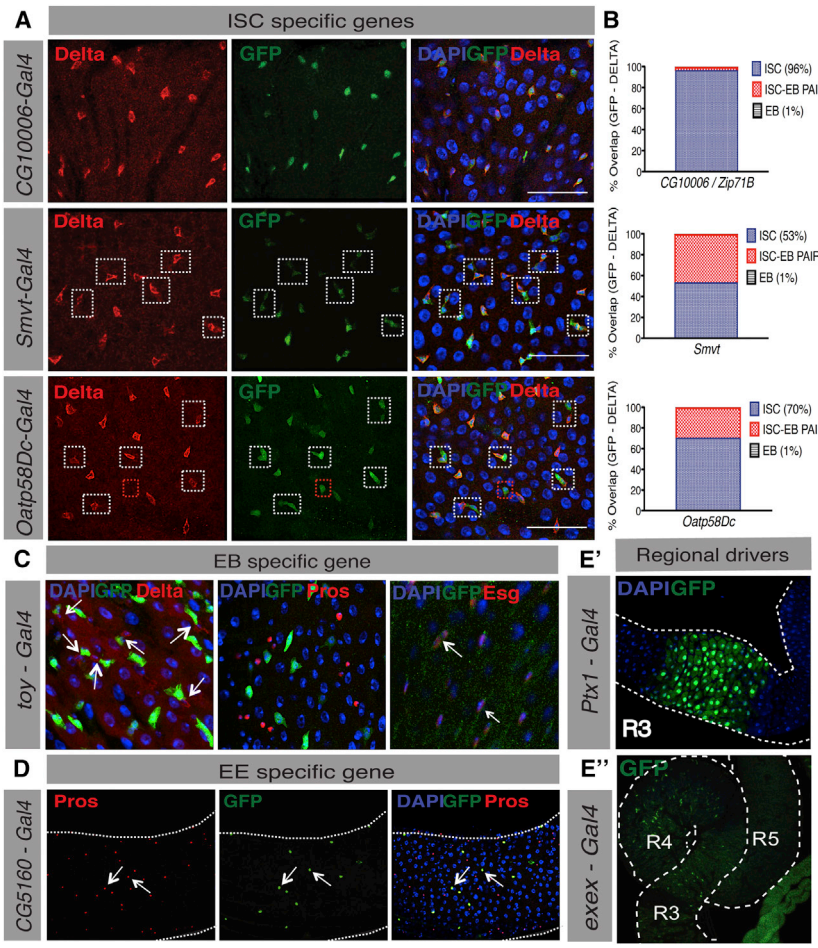

Figure 2. Novel Marker Genes and Role of *Smvt* in ISC Functionality

(A) Stem cell-specific transporter genes: *CG10006*, *Smvt*, and *Oatp58DC*. GFP showing co-localization with Delta antibody. Gal4 lines specifically mark ISCs and ISC-EB pairs. Boxes show ISC-EB pairs. The red box shows rare GFP$^+$ EB cell. Scale bar, 50 μm.

(B) Quantification of ISCs and ISC-EB pairs for *CG10006, Smvt*, and *Oatp58Dc*.

(C) *Toy* specifically marks EBs in the midgut. *toy-Gal4-UAS-GFP* marks cells having small nuclei that are negative for Delta and Prospero. Arrows showing Delta-negative EBs adjacent Delta-positive ISCs in ISC-EB pairs.

(D) CG5160 specifically marks a fraction of EEs and co-localizes with Prospero.

(E′) *Ptx1 Gal4* is expressed in R3 cells.

(E′′) *exex Gal4* is expressed in cells of R1–R4, but not R5.

be a prerequisite for differentiation. We identified 177 EB-high genes, including *twin of eyeless* (*toy*), *tor*, and *Ptth*. 226 genes, including neuropeptides *Tk* and *DH31*, were temporarily repressed by at least 2-fold in EBs as compared to ISCs and ECs (Table S1).

Altogether, our expression profiling showed that the *Drosophila* midgut is a transcriptionally diverse tissue and characterized differentiation as a complex process involving progressive changes in gene expression from stem cells to differentiated cells. It is noteworthy that the EB, typically viewed as a transient intermediate cell type, displayed a distinct, unique transcriptional profile.

Identification of Markers and Their Functions in the Midgut

To find additional drivers and markers for intestinal cells, we screened GAL4 enhancer traps of genes identified as cell-type specific by our FACS/RNA-seq analysis. By this approach, we identified the transporters *Zip71B/CG10006*, *Smvt* (primarily a biotin transporter), and *Oatp58Dc* as specific markers for ISCs and ISC-EB pairs, suggesting specific metabolic requirements for ISCs (Figures 2A and 2B). The *toy-Gal4* enhancer trap specifically marked cells having small nuclei, adjacent to *Delta*$^+$ ISCs in the newly formed ISC-EB pairs. These cells were negative for *Delta* and *Pros* but positive for *esg*, confirming that *toy* specifically marks the EBs in the gut (Figure 2C). We validated *CG5160* (a GTPase) as an EE-specific gene that marks a fraction of *Pros*$^+$ cells (Figure 2D). *Slit*, the ligand for the ISC-specific receptor *Robo2/lea*, was highly enriched in EEs as reported previously (Table S1) (Biteau and Jasper, 2014). No specific Gal4 driver for ECs was found, as the expression of most Gal4 lines of EC-high genes partially overlapped with the VMs. *Ptx1-Gal4* was found to specifically mark cells of the copper cell region or R3, and *exex-Gal4* specifically marked progenitors and EEs of all regions but R5 (Figures 2E′ and 2E′′).

To study the function of the identified "ISC-high" genes, we silenced the expression of these genes using the conditional *esg-Gal4 tub-Gal80^{ts}* (*esg-Gal4^{ts}*) driver system, which allows the conditional induction of UAS-linked RNAi and a marker gene (UAS-GFP) in progenitor cells (ISCs and EBs; Jiang and Edgar, 2009). Infection with a low dose of the gut pathogen *Pseudomonas entomophila* stimulates ISC proliferation, which can be measured by quantifying the number of phospho-histone 3$^+$ (PH3$^+$) cells. Within 3 days of *Smvt* silencing (with two different *Smvt^{RNAi}* lines) using the *esg-Gal4^{ts}* driver, we observed a loss of *Delta*$^+$ ISCs (Figure S2A). Rounded GFP$^+$ progenitor-like cells were still present, which were both *Pdm1*$^-$ and *Pros*$^-$ (markers for ECs and EEs) (Figure S2B). To test if *Smvt*-depleted stem cells could respond to damage and stress, we infected *esg^{ts}* > *Smvt^{RNAi}* flies with *P. entomophila* for 2 days. Strikingly, these flies had shrunken midguts and were susceptible to infection (Figures S2C and S2E). Quantification of PH3$^+$ cells confirmed a lack of proliferative response (Figures S2C and S2D). Further, an increase in *Smvt* expression was also observed in ISCs upon infection (Figure S2F). Next, *Smvt^{RNAi}* was induced specifically in ISCs using an ISC-specific driver, *esg-Gal4; Su(H)Gal80, Gal80^{ts}*. Within 7 days of induction of *Smvt^{RNAi}*, a loss of ISCs was

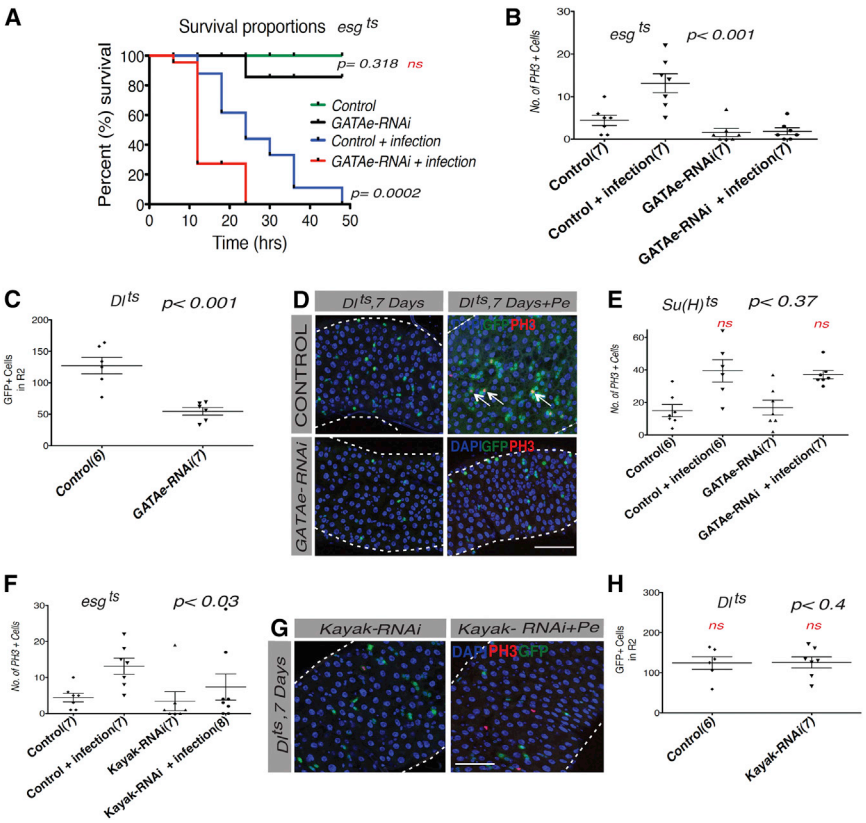

Figure 3. *GATAe* and *Kayak* Are Regulators of Stem Cell Maintenance and Regeneration in the Midgut

(A) Kaplan-Meier survival plot of *esg-Gal4^{ts}* flies expressing RNAi against *GATAe* upon infection with *P. entomophila* bacteria ($p < 0.0001$, log-rank [Mantel-Cox] test).

(B) Mitotic marker PH3^{+} counts confirming loss of regeneration in *esg-Gal4^{ts}* flies expressing *GATAe^{RNAi}* (n = 7).

(C and D) *GATAe* silencing in *Dl-Gal4^{ts}* flies causes reduction in the number of Delta^{+} ISCs (quantified in R2) and proliferative response upon infection.

(E) *GATAe* silencing in *Su(H)-Gal4^{ts}* flies does not inhibit proliferation or regenerative response upon infection (ns, not significant).

(F) PH3^{+} cell quantifications showing reduced regeneration potential in *esg-Gal4^{ts}* flies expressing RNAi against *Kayak*.

(G and H) *Kayak* silencing in *Dl-Gal4^{ts}* flies leads to reduced proliferative response to infection, without affecting number of Delta^{+} ISC (quantified in R2).

observed, specifically in R1 and R5 (Figure S2G). Conversely, silencing *Smvt* in *Su(H)*$^{+}$ progenitor cells led to a mild increase in proliferation, most likely due to cell stress in EBs, which in turn induced ISC proliferation. However, functional Delta^{+} ISCs were still present in these midguts, which could respond to infection (Figure S2H). Altogether, we identified cell- and regional-marker genes, and our results elucidated the crucial role of *Smvt* in maintaining functional ISCs and regulating midgut homeostasis.

The TFs *GATAe* and *Kayak* Regulate ISC Maintenance and Midgut Homeostasis

Next, as a potential way to find candidate TFs that might regulate ISCs, we used the i-cisTarget program (Herrmann et al., 2012) to identify TF binding sites enriched in the promoters of ISC-high genes (Table S1). In this gene set, we found enrichment for binding sites for the TFs *sna*, *kayak*, *Da*, *Ase*, *Iola*, *GATAe*, and *GATAd* (Table S4). Similarly, we identified transcriptional regulators of EB-, EC-, and EE-specific genes, some of which were also specifically expressed in the same cell types as their predicted targets, such as *toy* and *onecut* (Figure 2C; Table S5).

To test whether our predicted ISC regulatory TFs are important for ISC function, we first depleted several of them in ISCs and EBs using an *esg-Gal4^{ts}* driver and RNAi. After 7 days of expressing two different RNAi constructs against *GATAe* and 24 hr of *P. entomophila* infection, mortality of flies expressing *GATAe^{RNAi}* increased relative to controls (Figure 3A), with a significant decrease in the regenerative response (Figure 3B). We observed no effect of RNAi against *GATAd*, indicating that *GATAe* is the principle GATA factor required for midgut regeneration (data not shown). *GATAe^{RNAi}* was then induced separately in ISCs and EBs using the *Delta-Gal4 tub-Gal80^{ts}* (*Delta-Gal4^{ts}*), *esg-Gal4; Su(H)Gal80 Gal80^{ts}*, or *Su(H)-Gal4 tub-Gal80^{ts}* (*Su(H)-Gal4^{ts}*) driver lines (specific to ISCs and EBs, respectively). Upon silencing *GATAe* with *Delta-Gal4^{ts}* for 7 days, reduced number of GFP^{+} ISCs and a drop in the regenerative potential upon infection was observed (Figures 3C, 3D, and S3A). Induction of *GATAe^{RNAi}* under the control of *Su(H)-Gal4^{ts}* also caused GFP^{+} cell loss, although these flies displayed a normal regenerative response upon infection (Figures 3E, S3B, and S3C).

Upon expressing RNAi against *Kayak* under *esg-Gal4^{ts}* or *Delta-Gal4^{ts}* flies for 7 days, we observed a reduced proliferative response to infection, although the number of GFP^{+} ISCs remained unchanged (Figures 3F–3H). Altogether, these results demonstrate that *GATAe* acts in a cell-autonomous manner to regulate ISC maintenance and that both *Kayak* and *GATAe* have essential cell-autonomous functions in ISCs during midgut homeostasis and regeneration.

Snail Regulates ISC Proliferation and Progenitor Differentiation

Sna is a Snail family TF that was predicted by i-cisTarget as a potential regulator of ISCs. Using a *sna-LacZ* reporter line, we first confirmed *sna* to be expressed specifically and primarily in R3, R4, and R5 ISCs and also in newly formed ISC-EB pairs (Figures 4A and 4B). While *sna* was highly expressed in ISCs, it also showed relatively high expression in EBs (Figure 4B). Co-staining for *Su(H)*, *Snail-LacZ*, and *Delta* revealed the existence of cells (always in ISC-EB pairs) that were positive for all three markers,

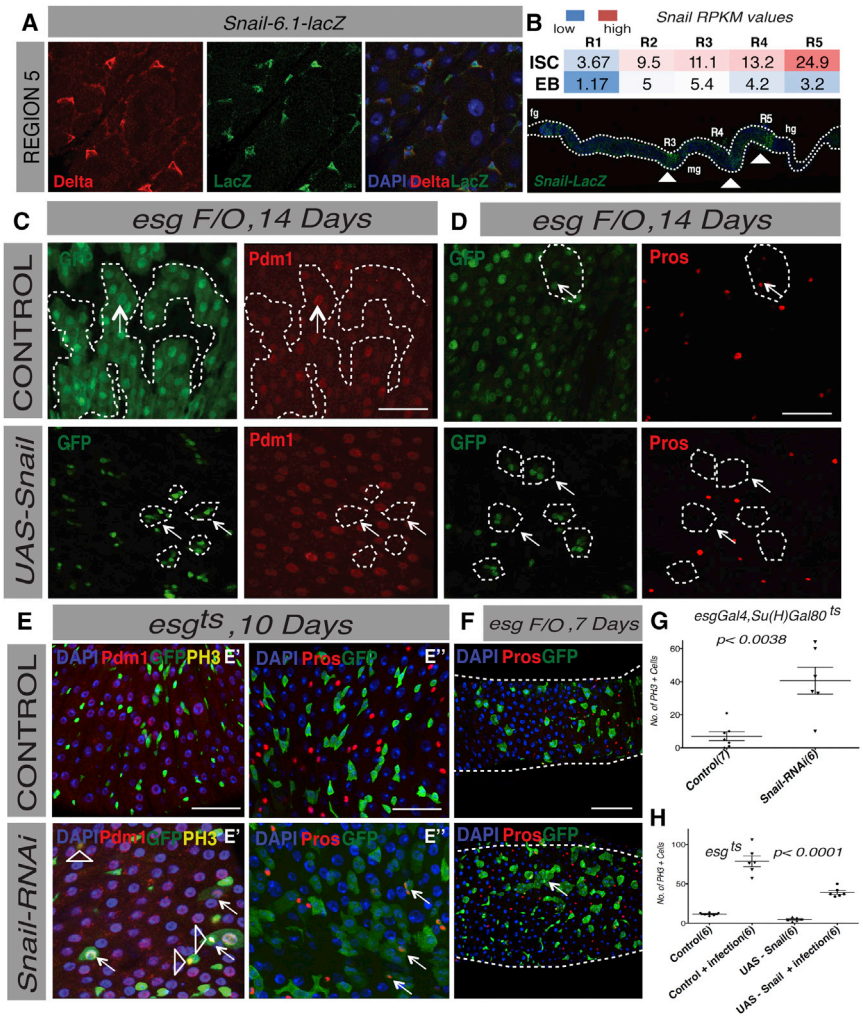

Figure 4. *Sna* Regulates ISC Proliferation and Progenitor Differentiation

(A) *sna-6.1-lacZ* specifically marks ISCs and ISC-EB pairs.

(B) *sna* is highly expressed in ISCs of R3, R4, and R5. EBs express considerably high levels of *sna*.

(C and D) Induction of UAS-*sna* in esg F/O flies abolishes differentiation and leads to formation of *Pdm1*$^-$, *Pros*$^-$ three- to four-cell clusters. Full arrows showing UAS-*sna* cell clusters negative for *Pros* and *Pdm1*.

(E) *esg-Gal4*^{ts} > *Sna*^{RNAi} flies have GFP$^+$ and Pros$^+$, Pdm1$^+$ cells. Empty arrowheads show PH3$^+$cells (scale bar, 50 μm).

(F) *sna*^{RNAi} induction in esg F/O flies for 7 days leads to bigger cell clusters (scale bar, 25 μm).

(G) Quantification of PH3$^+$ cells shows that silencing of *sna* in *esg-Gal4; Su(H)Gal80, Gal80*^{ts} flies leads to higher proliferation rates ($p < 0.0038$, Student's t test with Welch's correction).

(H) Overexpression of *sna* in ISCs leads to slowly dividing three- to four-cell cluster; however, ISCs are still responsive to infection stress (n = 6).

confirming previous reports (Bardin et al., 2010; Ohlstein and Spradling, 2007), indicating that *Delta* expression is maintained in early EBs (Figure S4A). *sna* expression was found to be downregulated in ISCs and EBs upon infection (Figure S4D). Expression of *sna* also progressively decreases from ISCs to EBs to ECs, suggesting that *sna* may need to be downregulated for differentiation (Table S3). Consistent with this notion, overexpression of *sna* specifically in EBs for 5 days using *Su(H)-Gal4*^{ts} led to increased numbers of Su(H)$^+$ cells (Figure S4B). We further used the *esg*$^{F/O}$ lineage-tracing system to drive *UAS-sna*, thus locking *sna* expression "on" in the ISC lineage. After 14 days of *UAS-sna* induction under *esg*$^{F/O}$ control, clusters (clones) of three to four small cells formed that were negative for differentiation markers of both ECs (*Pdm1*) and EEs (*Prospero*; Figures 4C and 4D). Thus, enforced *sna* expression completely blocked the differentiation of progenitor cells. These midguts also had reduced cell proliferation compared to controls and isolated *Delta*$^+$ ISC cells were observed, whereas control guts typically had two or more *Delta*$^+$ ISCs in each cluster (Figures 4H and S4C). Upon infection with *P. entomophila*, flies overexpressing *sna* could still respond by increasing the ISC division rate, indicating that these cells were viable and retained stem cell behavior (Figure 4H). Conversely, *sna* silencing using *esg-Gal4*^{ts} or *esg-Gal4; Su(H)Gal80, Gal80*^{ts} (ISC driver) flies for 10 days led to an increase in *Delta*$^+$ cells (Figure S4F) and ISC proliferation rates (Figures 4E″, 4G, and S4E). Regular cellular architecture as observed with Armadillo staining became aberrant in *sna*-depleted midguts (Figure S4G). Many *esg*$^+$ *Pdm1*$^+$ and *esg*$^+$ *Pros*$^+$ double-positive cells were observed, suggesting that loss of *sna* in EBs may lead to precocious differentiation (Figures 4E′ and 4E″). After 7 days of *sna*^{RNAi} induction by *esg*$^{F/O}$, clusters of nine or ten cells were formed as compared to clusters of two or three cells in controls (Figure 4F), indicating increased ISC proliferation. It remains to be determined whether this increase in proliferation upon *sna* silencing is a direct cell-autonomous effect in ISCs or the indirect consequence of a stress response triggered by loss of *sna*.

Intestinal Stem Cells Are Regionally Specialized

Hierarchical clustering of ISCs across midgut regions revealed that R1 ISCs (which included some type I GaSCs) and R3 ISCs (the type II GASCs) were quite distinct from the ISCs of R2, R4, and R5 (Figure 5A). Expression of all ISC-high genes, including the Notch ligand *Delta* and *sna*, varied in ISCs along the midgut by ~1.5- to 2-fold, and 920 genes showed regional variation in expression in ISCs (Figure 5C). GO analysis of these genes revealed strong enrichment for genes involved in transmembrane transport, ATP-hydrolysis-coupled proton transport, and proteolysis (Table S6). Key genes in those categories, such as vacuolar H$^+$ ATPases, were found to be R3

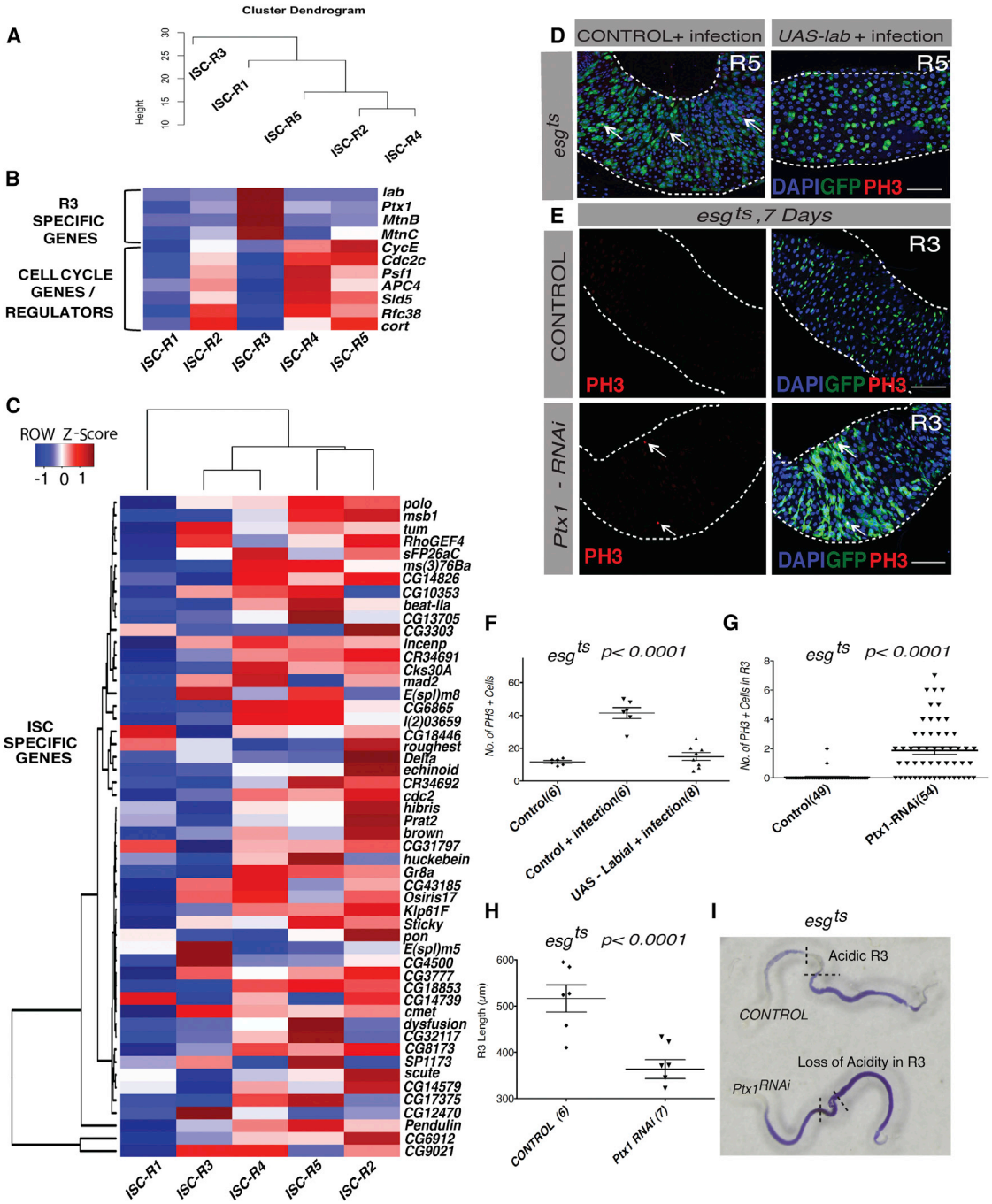

Figure 5. Distinct Specificities of ISCs Influence Regional Behavior

(A) Cluster dendogram of ISCs in regions R1–R5. R1 and R3 ISCs are distinct from other regions.

(B) Expression of regulatory genes across regions. *lab* and *Ptx1* are highly expressed in R3 ISCs, and cell-cycle genes are weakly expressed in R3.

(C) Expression of (showing top 50) stem cell-specific genes varies across regions.

(D) *lab* overexpression in *esg-Gal4*^{ts} flies partially abolishes regenerative response in flies upon infection.

(E) *Ptx1* silencing in *esg-Gal4*^{ts} flies accelerates proliferation of R3 ISCs, causing full renewal of the R3 region as compared to R3 in control flies (scale bar, 25 μm).

(F) Quantification of PH3^{+} cells upon *Labial* overexpression.

(G) PH3^{+} cell quantification in R3 of *esg-Gal4*^{ts} > *Ptx1*^{RNAi} flies ($p < 0.0001$, Student's t test with Welch's correction).

(H) Length of R3 region decreases upon *Ptx1* silencing (n = 6–7).

(I) *Ptx1* silencing in *esg-Gal4*^{ts} flies leads to loss of R3 acidity as shown by bromophenol blue staining.

specific (>3- to 12-fold as compared to other regions), the most acidic compartment of the midgut, suggesting a specialization of R3 ISCs to their physiological function (Table S6). We successfully validated the regional expression of a number of ISC-high genes using Gal4 enhancer trap lines and GFP gene traps. These included *sna*, *polo*, *Smvt*, *Oatp59Dc*, and *mira* (Figure S5A).

Pro-proliferative components of the EGFR and JAK-STAT pathways were found to be most highly expressed in R2, R4, and R5 ISCs, suggesting that quantitative differences in activity of these pathways could account for regional differences in ISC proliferation (Figure S5B). R3 ISCs also expressed low levels of cell-cycle regulatory genes, such as *cdc2c*, *Psf1*, *Sld5, Rfc38*, and *cort* (Figure 5B), accounting for their quiescent nature. Interestingly, they also expressed high levels of the regionalized TFs *labial* (*lab*) and *Ptx1*, suggesting that these TFs might directly modify the regional properties of R3 ISCs (Figures 2E′ and 5B).

As *Delta*$^{+}$ ISC numbers are low in R3, we used the *esg-Gal4*^{ts} instead of the *Dl-Gal4*^{ts} driver for functional tests of *lab* and *Ptx1*. Ectopic expression of *UAS-lab* in *esg-Gal4*^{ts} flies led to a partial loss of regenerative capacity in all midgut regions after *P. entomophila* infection, suggesting that *lab* overexpression in ISCs outside R3 could block proliferation (Figures 5D and 5F). Knockdown of *lab* by RNAi in progenitor cells did not change regional identity or turnover rates in R3 (data not shown). In contrast, silencing *Ptx1* by expressing RNAi using the *esg*$^{F/O}$ or *esg-Gal4*^{ts} systems led to accelerated ISC proliferation and epithelial renewal in R3 (Figures 5E, 5G, and S5C). No increase in proliferation was observed in R3 upon expression of *Ptx1*^{RNAi} specifically in ECs, confirming that loss of *Ptx1* accelerates proliferation in R3 by acting autonomously in progenitors (Figures S5E and S5F). Curiously, the R3 region was also shortened in *Ptx1*^{RNAi}-expressing flies, and bromophenol blue staining revealed a complete loss of R3 acidity (loss of yellowish color) upon *Ptx1* silencing in both *Myo1A-Gal4*^{ts} and *esg-Gal4*^{ts} flies (Figures 5H, 5I, and S5D) indicating a role of *Ptx1* in the normal function of the R3 region. Altogether, our results confirm that the R3-specific TFs *Ptx1* and *lab* modulate the regional properties of R3 ISCs in the region.

The Transcriptomes of Differentiated ECs, EEs, and EBs Vary by Midgut Region

Transcriptomes of differentiated epithelial cells (ECs and EEs) displayed more regional variation in expression than progenitor cells, consistent with their varied morphology (Figures 6A, S6A, and S6B). We examined cell-specific expression of digestive enzymes and nutrient transporters and found some of them to be cell-type and regionally specific, mainly in the differentiated ECs, EEs, and VMs. (Figure 6B). While glycoside hydrolases like *Amy-d*, *Hexo1*, *Cda9*, and lipase *CG6271* were primarily expressed in R1 and R3, serine type peptidases like *Fur1*, *Jon44E*, and *Ser6* were highly expressed by the ECs, EEs, and VMs of R4 and R5 (Figure 6B). Glucose transporter *Glut1* was expressed in R1 VMs, ECs, and EEs, and amino acid transporters *NAAT1* and *EAAT1* were expressed primarily in VMs of R1 and R5.

Genes that varied regionally in ECs were enriched in 31 biological process GO terms including ATP-dependent proteolysis and aminoglycan metabolic process (Figure 6B; Table S6). Genes involved in immune regulation are also strongly patterned, especially in enterocytes (Buchon et al., 2013a). Likewise, genes encoding peptidoglycan recognition proteins (PGRPs) displayed high regional specificity. For instance, PGRP-SD was primarily expressed in R1 and R4, whereas expression of PGRP-SC1a was highest in R3 and R4, indicative of regionalized regulation of immune defense in the gut (Figure 6C).

EEs showed particularly strong differences in expression by region (Figures 6A, 6D, and S6A). 35 biological process GO terms were significantly enriched among differentially expressed genes in EEs across regions. These included the transmembrane transport-GPCR signaling pathway and humoral immune response (Table S6). We detected a patterned expression of all known neuropeptide hormones, including *Tk*, *Dh31*, *Ast-A*, *Mip*, *NPF*, *Bursicon*, and *CCHamide-1*, *2*, along the gut (Veenstra et al., 2008; Scopelliti et al., 2014) (Figure 6D). In agreement with our genomic data, *Tk-Gal4* displayed a distinct regionalized expression pattern (compare Figure 6D and Figure S6C). Hormones not previously detected in the gut, such as *CCAP*, were also expressed specifically in EEs (Table S1).

Genes differentially expressed in EBs across regions showed 72 enriched GO functions. These included "open tracheal system" and "regulation of anatomical structure size" (Table S6). These results show that each midgut cell population has its own exclusive regional expression pattern. Interestingly, some consistency was observed among the genes that were regionally expressed in progenitors and differentiated cells for each region, suggesting that regionality might be inherited through the stem cell lineage or regional identity could be coordinated by positional cues.

VM Cells Express Growth Factors in a Region-Specific Manner

Remarkably, mesodermally derived VMs were the most variable in gene expression across midgut regions as compared to other cell types (Figure S1A; Table S6). 108 biological process GO terms, including regulation of hormone levels and digestive tract development, were significantly enriched among the genes differentially expressed by region in VMs (Table S6). Notably, the morphogens *Wnt1/wg*, *Wnt4*, *Wnt6*, and *WntD* had their highest expression in VMs and were expressed in gradients, primarily in R1 and R5, in agreement with a previous study on gut regionalization (Figure S6D; Buchon et al., 2013a). The EGFR ligand *Vn*, involved in ISC proliferation, was preferentially expressed in the VMs of R4 and R5, the most proliferative regions of the gut (Figure 6E). The morphogen *Dpp* was specifically expressed in the VMs in a regionalized manner (Figure 6E). These results illustrate that paracrine signals from VMs differ quantitatively and qualitatively between different regions, suggesting that these could modulate regional identity and cell behavior along the gut.

Infection Induces Massive Transcriptional Responses in Midgut Cells

Infection massively alters gut structure, and this confounded our attempts to sort cells from specific regions. Instead, we monitored changes in the transcriptome of each cell type FACS

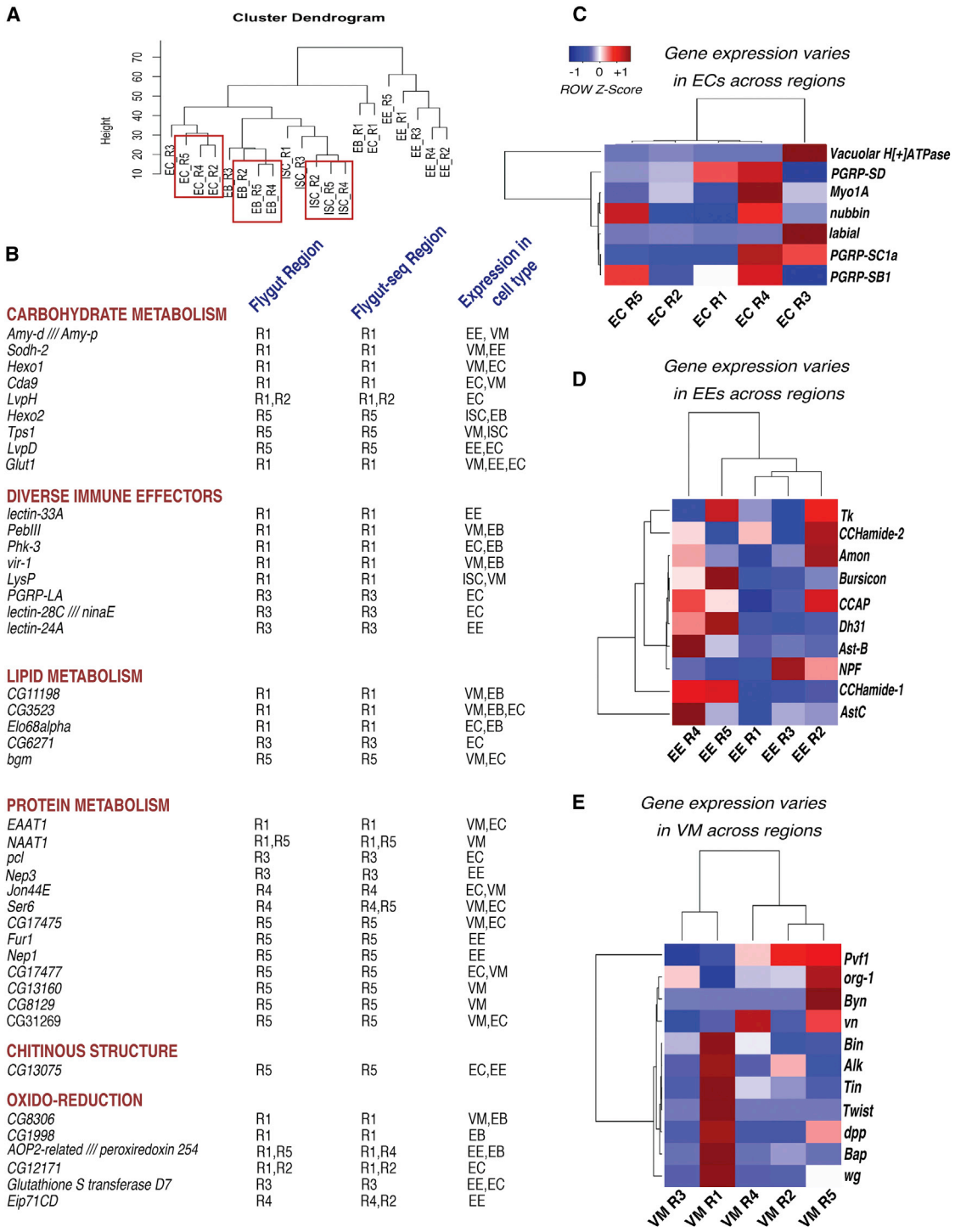

Figure 6. Midgut Cells Are Regionally Distinct and Engender Diversity in Midgut Regions

(A) Dendogram showing relationship of midgut cells of different regions.

(B) Regionally specialized genes involved in digestion are expressed cell-type specifically.

(C) Heatmap of EC-specific genes and PGRPs.

(D) Heatmap of EE-specific hormones.

(E) Heatmap of VM specific genes across regions (scale bar, normalized expression values increasing from blue to red). Scaling of matrices by row to a mean of zero and SD of one (Z score normalization) shows relative expression patterns.

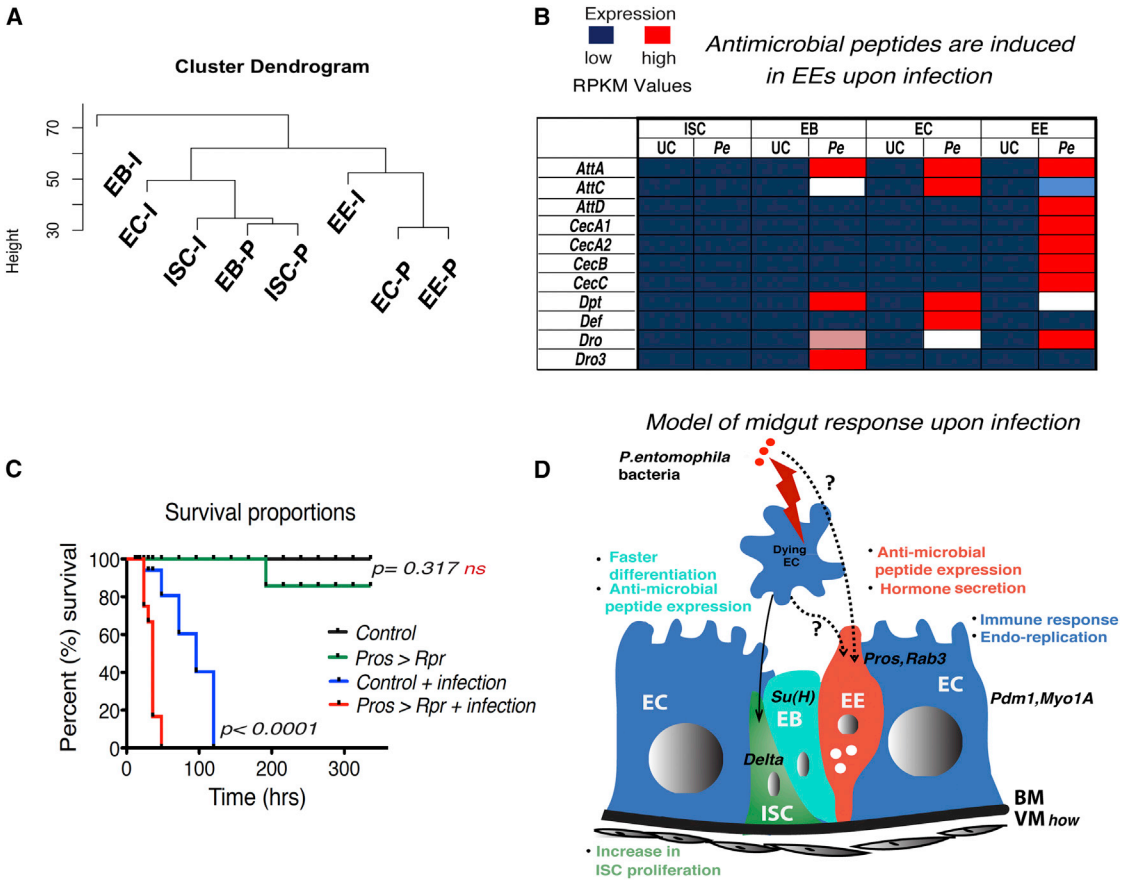

Figure 7. Cell-Type-Specific Responses upon Infection with *P. entomophila*

(A) Cluster dendogram showing infection leads to huge cell-type-specific responses. I, infected; P, physiological.

(B) Antimicrobial peptide (AMP) expression increases in EEs upon infection (UC, unchallenged; Pe, *P. entomophila*). Scale bar, normalized expression values increasing from blue to red.

(C) Kaplan-Meier survival plot showing EE-depleted flies have higher susceptibility to infection as compared to controls ($p < 0.0001$, log-rank [Mantel-Cox] test, 3 × 15 animals/genotype).

(D) Model of intestinal response upon *P. entomophila* infection.

sorted from whole midguts following enteric infection with *P. entomophila*. Rapid epithelium renewal following infection is expected to change the specificity of our GFP cell markers, since GFP is a relatively stable protein and is transmitted to daughter cells following ISC division. To minimize this problem, we sorted cells both based on GFP marker expression and cell size (see Experimental Procedures). Genes involved in cell-cycle progression (*polo*, *cdc2*, *tum*, and *Cks30A*) and the ISC marker *Delta* remained expressed in ISCs and were not highly expressed in EBs. Similarly, *pros* and *Rab3* remained EE specific and *toy* remained EB specific (Figure S6E; Table S7), indicating that our sorting method did not grossly compromise cell specificity.

Across all cell types, a total of 6,734 genes were differentially expressed after infection by *P. entomophila*, indicating that infection leads to a massive shift in the midgut transcriptional landscape (Table S7). GO enrichment analysis indicated that expression of genes involved in cell differentiation (*pros*, *nubbin*, *pdm2*, and *pdm3*), transport (*Smvt* and *ABCB7*), and antimicrobial peptides (AMPs; *AttA*, *AttC*, and *CecA2*; Table S8) were among the most affected. 1,833 genes were differentially expressed in ISCs and 2646 in EBs. ECs and EEs also displayed significant responses, but to a lesser extent, with 233 and 453 genes differentially expressed, respectively (Figure 7A). In ECs, infection altered the expression of genes involved in ribosome biogenesis, transport, DNA repair, and DNA replication genes like *Fen1*, *Pms2*, and *Rad9* and immunity effectors like *AttD* and *PGRP-SB1* (Tables S7 and S8). This is in agreement with our data showing that new ECs endocycle upon infection to grow, generating larger cells than at homeostasis (B.A.E. and J. Xiang, unpublished data).

While ECs are known to be the front line in immune defense (Miron and Cristea, 2012), expression of many AMPs was strikingly induced in EEs upon infection (Figure 7B). Some of these AMPs were much more strongly induced in EEs, whereas others were more highly induced in ECs or EBs, suggesting cell-type-specific regulation of the immune response (Figure 7B). To test whether EEs are important in responding to pathogens, we ablated them by expressing *UAS-rpr* (*Reaper*) for 3 days with

the EE-specific Gal4 driver *Pros-v1-Gal4^{ts}*. While unchallenged EE-depleted flies survived for at least 15 days, they were more susceptible to *P. entomophila* infection than controls (Figure 7C). Upon infection, EBs also produced AMPs and specifically activated genes involved in organ development (e.g., *abd-A*, *Actin57B*, and *ao*), consistent with a dual role in the immune response and in the direct reconstruction of the tissue (Tables S7 and S8). ISCs did not seem to contribute to the production of immune effectors. Altogether, these results show that infection generates massive changes in transcription in all cell types, ranging from ISC activation and immune induction in EBs, ECs, and EEs to hormonal alterations.

DISCUSSION

A Unique ISC-Specific Gene Repertoire Associated with Stemness

In our analysis, we uncovered genes highly expressed in ISCs and identified enriched *cis*-regulatory motifs upstream of these "ISC-high" genes. This approach identified *GATAe*, *sna*, *Fos* (*Kayak)*, and *Ptx1* as central regulators of ISC behavior and paved the way for future studies on more factors that could influence ISC functionality. We confirmed *sna* as a regional ISC-high gene that regulates stem cell differentiation in the midgut similar to its paralog, *escargot* (*esg*) (Korzelius et al., 2014). In contrast, *GATAe* functions in ISC maintenance, much like its mammalian homolog, *GATA6*, which is involved in the maintenance and proliferation of stem cells and colorectal cancer (Beuling et al., 2012; Whissell et al., 2014). *Kay* (the fly homolog of *Fos*) and *Da* had previously been identified as TFs that control ISC activity and fate (Biteau and Jasper, 2011; Bardin et al., 2010). Thus, our results indicate that stem cell activity is controlled not by a single factor but by a combinatorial network of autonomously acting TFs such as *GATAe*, *kayak*, and *sna* and previously studied *da*, *esg*, and *sc*, which in concert regulate stemness in the midgut. This dataset could be a useful resource for identifying mammalian homologs with similar functions in stem and cancer cells and in understanding TF regulatory networks in mammals.

The primary source of biotin for *Drosophila* is dietary yeast and enteric bacteria. Interestingly, we show that the biotin transporter *Smvt* (Camporeale et al., 2007) is essential for ISC maintenance and homeostasis, signifying the importance of nutrients derived from symbiotic organisms in regulating intestinal homeostasis and ISC function (Buchon et al., 2009, 2013b).

Regional Cell Specialization Influenced Regional Form and Function

An evolutionarily conserved feature of the gastrointestinal tract is the division of function between specialized regions. Our study reveals that all cell types of the *Drosophila* midgut have profound regional variation in their gene expression. Nevertheless, differences between intestinal cell types were even more pronounced than regional variations within a specific cell type (Figure 1B). For all cell types, we consistently found the cells of regions R1 and R3 to be vastly different from those of the other regions (Figures 1B and S6A). This suggests that the specialization of all cells in a region is coordinated.

In the gut epithelium proper, differentiated cells showed the most regionalization, with EEs being the most variant between regions. In agreement with recent studies documenting enteroendocrine cell diversity in the midgut (Beehler-Evans and Micchelli, 2015; Veenstra et al., 2008), our results indicate that there are multiple subtypes of the hormone secreting EEs that likely have regionalized functions. EBs and ECs also showed clear regional specificities, including altered expression of genes involved in metabolism and digestion. Although lipases, glycoside hydrolases, and glucose transporters were highly expressed in the anterior midgut, serine endopeptidases and amino acid transporters were primarily expressed in the posterior midgut cells, consistent with the premise that digestion is highly compartmentalized (Buchon et al., 2013a; Marianes and Spradling, 2013).

Remarkably, multipotent ISCs also displayed transcriptional variation along the length of the gut. Different ISC populations differ in the levels of effectors and targets in key signaling pathways, such as EGFR/Ras/MAPK, Wnt, and JAK/STAT, also showing distinct qualitative differences. Of note, ISCs of the acidic R3 express vacuolar H^+ ATPases, indicating an adaptation of ISCs to their local environment. Our tests showed that the R3-specific TFs *Ptx1* and *lab* are important for maintaining these regional ISC regional properties. We identified additional regionalized TFs like *exex* and *Drm*, and some of these are likely to control other regional properties. While regionalized gene expression almost certainly determines regional differences in cell morphology and function, enteric environment factors (e.g., microbiota and nutrition distributions) within the gut might also influence regional characteristics.

The transcriptome of visceral muscles varied strongly by region, and studies have suggested that regional identities in the gut are maintained by gradients of morphogens (Buchon et al., 2013a; Li et al., 2013). Accordingly, the morphogens *Wg*, *Wnt 4, Wnt 6*, *WntD*, *Dpp*, and *Vn* were expressed in gradients in VM cells, suggesting roles for these components of the stem cell niche in defining a region's transcriptional signature. However, we noticed that spatial expression of lowly expressed ligands like *Dpp* and *Upd3* varied from previous reports (Jiang et al., 2009; Tian and Jiang, 2014), and thus, this dataset should be used with discretion in such cases. Solely based on gene expression data, we cannot determine whether the ISCs or niche cells such as VMs are primary in establishing and maintaining regionalization. It will be interesting to test whether differences in the niche are driven by gut-extrinsic factors or whether ISCs engineer their own niche through self-reinforcing feedback, for instance, by epigenetic programming of daughter cells. We hope that our data will guide future experiments that test the cross-talk between stem cells and the niche in midgut regionalization.

Differentiated EEs and ECs Combat Enteric Infection

We uncovered an unexpected role for EEs as potential players in the immune response to pathogens by inducing AMP expression along with ECs and EBs. Interestingly, the different cell types produce different combinations of AMPs, suggesting a specialization by cell type in the immune response, as also found in the mammalian digestive tract (Peterson and Artis, 2014). We propose a model (Figure 7D) wherein infection either directly

activates EEs to express AMPs or the damaged ECs signal ISCs to proliferate and EEs to produce AMPs. Further studies will be required to clearly define the response of EEs to infection.

In conclusion, we have systematically characterized transcription by genomic analysis of regions and cell types in the *Drosophila* midgut. Gut regionalization is a critical factor for human health, as diseases of intestinal origin are often regionalized. We hope that the dataset we provide (http://flygutseq.buchonlab.com/) will help to pave the way for future studies that elucidate the complex interplay among midgut cells, regions, and microbes that will promote our understanding of gut physiology and homeostasis.

EXPERIMENTAL PROCEDURES

Fly Strains and Crosses

Flies for all experiments were maintained at 18°C or 25°C. 7- to 10-day-old female flies were used for all expression profiling experiments. Flies were shifted for 3 days to 29°C prior to dissection and FACS sorting. The following fly lines were used to select different cell populations: *esg-Gal4 UAS-GFP; tub-Gal80ts* (ISCs and EBs), *Dl-Gal4 UAS-CD8-GFP* (ISCs), *Su(H)GBE-Gal4 UAS-GFP; tub-Gal80ts* (EBs), *Myo1A-Gal4; tub-Gal80ts UAS-GFP* (ECs), *How-Gal4 UAS-GFP; tub-Gal80ts* (VM), and *Rab3-YFP* or *tub-Gal80ts UAS-GFP; Pros-v1-Gal4* for (EEs).

For functional tests we used the following genotypes: *Dl-Gal4 UAS-GFP; tub-Gal80ts* or *esg-Gal4 UAS-GFP; tub-Gal80ts Su(H)GBE-tub-Gal80* (for ISCs), *w; UAS-Snail*; *Tk-Gal4*; VDRC stocks $Smvt^{RNAi}$ - v102662, v40650; $Snail^{RNAi}$ - v6232, v50004; $Ptx1^{RNAi}$- v10778, and v19831; and Bloomington TRiP lines $GATAe^{RNAi}$ - 33748, 34641 and 34907; $Labial^{RNAi}$- 26753.

RNA Sample Preparation for Sequencing

For region-specific cell-type profiling, individual regions were dissected and dissociated as described in Dutta et al. (2013). Briefly, 100–150 guts were dissected in RNase-free PBS and dissociated for 45 min to 1 hr using 100 μl elastase (4 mg/ml stock) in 400 μl PBS (final concentration 0.8 mg/ml) at 27°C with frequent pipetting. Different filter sizes were used (25 μm for ISCs, 40 μm for EBs and EEs, 70 μm for ECs, and 100 μm for VMs. Cells were then sorted based on intensity of marker expression using FACS Aria III (BD Biosciences), with 85- to 100-μm nozzle sizes. More than 2,000 cells were sorted for cell-type-specific profiling. Visceral muscle cells are large syncytia; hence, a longer and more vigorous treatment with 150 μl elastase was done for 1.5–2 hr for each region. Cells were sorted straight into RNA extraction buffer. Extracted RNA was amplified as described previously (Dutta et al., 2013), converted to cDNA, and sequenced using an Illumina HiSeq2000 machine. The RNA-seq protocol is detailed in the Supplemental Experimental Procedures.

Mapping, Quantification, and Visualization

Raw fastq reads were mapped to the *Drosophila* genome (*Drosophila*_melanogaster.BDGP5.70.dna.toplevel.fa) using Tophat 2.0.9, allowing two mismatches. Integrated Genomics Viewer was used to visualize mapped reads. Unmapped reads were discarded. Python package HTSeq version 0.5.4p5 was used to generate raw counts, and DESeq (p value adjustment 0.05 by the Benjamini-Hochberg method) was used for differential expression analysis.

cis-Regulatory Module Prediction

Regulatory elements and CRMs were predicted using the integrative genomics method i-cisTarget (Herrmann et al., 2012). Region mapping was set to default: 5 kb upstream, 5′ UTR, and first intron for prediction of potential transcriptional regulators.

Immunofluorescence and Gal4 Line Screen

After dissection and paraformaldehyde fixation, midguts were stained with antibodies as per standard protocols (Jiang et al., 2009). Gal4 enhancer traps were crossed to *UAS-nls-GFP* flies, and co-localization of GFP-marked cells and Delta- or Pros-positive cells was examined using a Leica SP5 (three biological replicates) to check for specificity of gene expression in cells. Source of antibodies used can be found in the Supplemental Experimental Procedures.

Survival Experiments and Mitotic Index

Adult flies were shifted to 29°C for 2–3 days before infection and flies were infected with *P. entomophila* for 48 hr. The number of living flies were counted roughly every 12–24 hr. Mitotic index was determined by counting the number of PH3-positive cells from 6–15 whole female midguts from three independent experiments.

Bromophenol Blue Staining

Flies were maintained on 0.3% bromophenol blue diet for 24 hr following 7 days induction of RNAi at 29°C on standard food.

Additional Methods

Details regarding mRNA sequencing, RPKM normalization, bacterial infection, FACS, and image analysis protocols are provided in the Supplemental Experimental Procedures.

ACCESSION NUMBERS

The data discussed in this publication have been deposited to the NCBI GEO and are available under accession number GEO:GSE61361.

SUPPLEMENTAL INFORMATION

Supplemental Information includes Supplemental Experimental Procedures, six figures, and eight tables and can be found with this article online at http://dx.doi.org/10.1016/j.celrep.2015.06.009.

AUTHOR CONTRIBUTIONS

D.D., B.A.E., and N.B. conceptualized the project and wrote the manuscript. D.D. and N.B. generated RNA-seq datasets. D.D. standardized FACS methods and performed validation experiments. A.J.D., C.G., D.D., and N.B. performed data analysis. P.L.H. and J.K. helped with experiments on *Ptx1* and *GATAe* and *Snail*. J.R. designed the Flygut-seq website. A.J.D. and P.H.P. gave valuable comments during the preparation of the manuscript.

ACKNOWLEDGMENTS

We thank Monika Langlotz and David Ibberson from University of Heidelberg for help with FACS and RNA sequencing. We are grateful to Maria Leptin, Norbert Perrimon, Craig Micchelli, Joaquin de Navascues, M. Gonzalez-Gaitan, James C Hombría, Steven Hou, Susan Eaton, and Huaqi Jiang for fly stocks and antibodies. Funded by DFG SFB873, DKFZ A220, and ERC Advanced Grant 26515 to B.A.E., and N.B. was supported by the Empire State Stem Cell Fund through New York State Department of Health NYSTEM contract C029542.

Received: October 9, 2014
Revised: April 2, 2015
Accepted: June 2, 2015
Published: July 2, 2015

REFERENCES

Amcheslavsky, A., Jiang, J., and Ip, Y.T. (2009). Tissue damage-induced intestinal stem cell division in Drosophila. Cell Stem Cell *4*, 49–61.

Anders, S., and Huber, W. (2010). Differential expression analysis for sequence count data. Genome Biol. *11*, R106.

Bardin, A.J., Perdigoto, C.N., Southall, T.D., Brand, A.H., and Schweisguth, F. (2010). Transcriptional control of stem cell maintenance in the Drosophila intestine. Development *137*, 705–714.

Beehler-Evans, R., and Micchelli, C.A. (2015). Generation of enteroendocrine cell diversity in midgut stem cell lineages. Development *142*, 654–664.

Beuling, E., Aronson, B.E., Tran, L.M.D., Stapleton, K.A., ter Horst, E.N., Vissers, L.A., Verzi, M.P., and Krasinski, S.D. (2012). GATA6 is required for proliferation, migration, secretory cell maturation, and gene expression in the mature mouse colon. Mol. Cell. Biol. *32*, 3392–3402.

Biteau, B., and Jasper, H. (2011). EGF signaling regulates the proliferation of intestinal stem cells in Drosophila. Development *138*, 1045–1055.

Biteau, B., and Jasper, H. (2014). Slit/Robo signaling regulates cell fate decisions in the intestinal stem cell lineage of Drosophila. Cell Rep. *7*, 1867–1875.

Buchon, N., Broderick, N.A., Chakrabarti, S., and Lemaitre, B. (2009). Invasive and indigenous microbiota impact intestinal stem cell activity through multiple pathways in Drosophila. Genes Dev. *23*, 2333–2344.

Buchon, N., Broderick, N.A., Kuraishi, T., and Lemaitre, B. (2010). Drosophila EGFR pathway coordinates stem cell proliferation and gut remodeling following infection. BMC Biol. *8*, 152.

Buchon, N., Osman, D., David, F.P.A., Fang, H.Y., Boquete, J.-P., Deplancke, B., and Lemaitre, B. (2013a). Morphological and molecular characterization of adult midgut compartmentalization in Drosophila. Cell Rep. *3*, 1725–1738.

Buchon, N., Broderick, N.A., and Lemaitre, B. (2013b). Gut homeostasis in a microbial world: insights from Drosophila melanogaster. Nat. Rev. Microbiol. *11*, 615–626.

Camporeale, G., Zempleni, J., and Eissenberg, J.C. (2007). Susceptibility to heat stress and aberrant gene expression patterns in holocarboxylase synthetase-deficient Drosophila melanogaster are caused by decreased biotinylation of histones, not of carboxylases. J. Nutr. *137*, 885–889.

Cordero, J.B., Stefanatos, R.K., Scopelliti, A., Vidal, M., and Sansom, O.J. (2012). Inducible progenitor-derived Wingless regulates adult midgut regeneration in Drosophila. EMBO J. *31*, 3901–3917.

Dimitriadis, V.K. (1991). Fine structure of the midgut of adult Drosophila auraria and its relationship to the sites of acidophilic secretion. J. Insect Physiol. *37*, 167–177.

Dutta, D., Xiang, J., and Edgar, B.A. (2013). RNA expression profiling from FACS-isolated cells of the Drosophila intestine. Curr. Protoc. Stem Cell Biol. *27*, Unit 2F.2.

Goulas, S., Conder, R., and Knoblich, J.A. (2012). The Par complex and integrins direct asymmetric cell division in adult intestinal stem cells. Cell Stem Cell *11*, 529–540.

Guo, Z., Driver, I., and Ohlstein, B. (2013). Injury-induced BMP signaling negatively regulates Drosophila midgut homeostasis. J. Cell Biol. *201*, 945–961.

Herrmann, C., Van de Sande, B., Potier, D., and Aerts, S. (2012). i-cisTarget: an integrative genomics method for the prediction of regulatory features and cis-regulatory modules. Nucleic Acids Res. *40*, e114.

Jiang, H., and Edgar, B.A. (2009). EGFR signaling regulates the proliferation of Drosophila adult midgut progenitors. Development *136*, 483–493.

Jiang, H., Patel, P.H., Kohlmaier, A., Grenley, M.O., McEwen, D.G., and Edgar, B.A. (2009). Cytokine/Jak/Stat signaling mediates regeneration and homeostasis in the Drosophila midgut. Cell *137*, 1343–1355.

Jiang, H., Grenley, M.O., Bravo, M.-J., Blumhagen, R.Z., and Edgar, B.A. (2011). EGFR/Ras/MAPK signaling mediates adult midgut epithelial homeostasis and regeneration in Drosophila. Cell Stem Cell *8*, 84–95.

Korzelius, J., Naumann, S.K., Loza-Coll, M.A., Chan, J.S., Dutta, D., Oberheim, J., Gläßer, C., Southall, T.D., Brand, A.H., Jones, D.L., and Edgar, B.A. (2014). Escargot maintains stemness and suppresses differentiation in Drosophila intestinal stem cells. EMBO J. *33*, 2967–2982.

Li, H., Qi, Y., and Jasper, H. (2013). Dpp signaling determines regional stem cell identity in the regenerating adult Drosophila gastrointestinal tract. Cell Rep. *4*, 10–18.

Lin, G., Xu, N., and Xi, R. (2008). Paracrine Wingless signalling controls self-renewal of Drosophila intestinal stem cells. Nature *455*, 1119–1123.

Marianes, A., and Spradling, A.C. (2013). Physiological and stem cell compartmentalization within the Drosophila midgut. eLife *2*, e00886.

Martorell, Ò., Merlos-Suárez, A., Campbell, K., Barriga, F.M., Christov, C.P., Miguel-Aliaga, I., Batlle, E., Casanova, J., and Casali, A. (2014). Conserved mechanisms of tumorigenesis in the Drosophila adult midgut. PLoS ONE *9*, e88413.

Micchelli, C.A., and Perrimon, N. (2006). Evidence that stem cells reside in the adult Drosophila midgut epithelium. Nature *439*, 475–479.

Miron, N., and Cristea, V. (2012). Enterocytes: active cells in tolerance to food and microbial antigens in the gut. Clin. Exp. Immunol. *167*, 405–412.

Ohlstein, B., and Spradling, A. (2006). The adult Drosophila posterior midgut is maintained by pluripotent stem cells. Nature *439*, 470–474.

Ohlstein, B., and Spradling, A. (2007). Multipotent Drosophila intestinal stem cells specify daughter cell fates by differential notch signaling. Science *315*, 988–992.

Peterson, L.W., and Artis, D. (2014). Intestinal epithelial cells: regulators of barrier function and immune homeostasis. Nat. Rev. Immunol. *14*, 141–153.

Scopelliti, A., Cordero, J.B., Diao, F., Strathdee, K., White, B.H., Sansom, O.J., and Vidal, M. (2014). Local control of intestinal stem cell homeostasis by enteroendocrine cells in the adult Drosophila midgut. Curr. Biol. *24*, 1199–1211.

Shaw, R.L., Kohlmaier, A., Polesello, C., Veelken, C., Edgar, B.A., and Tapon, N. (2010). The Hippo pathway regulates intestinal stem cell proliferation during Drosophila adult midgut regeneration. Development *137*, 4147–4158.

Singh, S.R., Zeng, X., Zheng, Z., and Hou, S.X. (2011). The adult Drosophila gastric and stomach organs are maintained by a multipotent stem cell pool at the foregut/midgut junction in the cardia (proventriculus). Cell Cycle *10*, 1109–1120.

Strand, M., and Micchelli, C.A. (2011). Quiescent gastric stem cells maintain the adult Drosophila stomach. Proc. Natl. Acad. Sci. USA *108*, 17696–17701.

Tian, A., and Jiang, J. (2014). Intestinal epithelium-derived BMP controls stem cell self-renewal in *Drosophila* adult midgut. eLife *3*, e01857.

Veenstra, J.A., Agricola, H.-J., and Sellami, A. (2008). Regulatory peptides in fruit fly midgut. Cell Tissue Res. *334*, 499–516.

Whissell, G., Montagni, E., Martinelli, P., Hernando-Momblona, X., Sevillano, M., Jung, P., Cortina, C., Calon, A., Abuli, A., Castells, A., et al. (2014). The transcription factor GATA6 enables self-renewal of colon adenoma stem cells by repressing BMP gene expression. Nat. Cell Biol. *16*, 695–707.

Zeng, X., and Hou, S.X. (2015). Enteroendocrine cells are generated from stem cells through a distinct progenitor in the adult Drosophila posterior midgut. Development *142*, 644–653.